Volcanic Hazards at the Proposed Yucca Mountain, Nevada, High-Level Radioactive Waste Repository II: Probabilistic Analysis

Charles B. Connor, Brittain E. Hill, Budhi Sagar

Center for Nuclear Waste Regulatory Analyses, Southwest Research Institute, San Antonio, TX

John Trapp

U.S. Nuclear Regulatory Commission, Office of Nuclear Materials Safety and Safeguards, Division of Waste Management, Washington, DC

Abstract. The probability of volcanic eruptions through the proposed Yucca Mountain high-level radioactive waste repository is estimated to be 10^{-8} - 10^{-7}/yr, approximately one order of magnitude greater than average rates of volcanic activity in the western Great Basin. These results are based on application of Gaussian and Epanechnikov kernels to the probability analysis, parameter estimation based on distribution of existing vents, vent alignment development in the Yucca Mountain region, and structural controls on patterns in basaltic volcanism. Integration of these factors yields hazard estimates greater than previous estimates [*Connor and Hill*, 1995] and at the high end of previously proposed ranges (i.e., 1×10^{-10} - 4×10^{-8}/yr) [*DOE*, 1998], chiefly because of the location of the proposed repository within a broad crustal density low produced by a half-graben. Modification of Gaussian and Epanechnikov kernel functions to include this geological structure, which appears to have controlled past volcanic activity, provides a mechanism to link patterns in basaltic volcanism and crustal

extension in a quantitative analysis for the first time. This technique may be widely applicable to assessment of volcanic hazards resulting from small-volume basaltic volcanic fields.

Introduction

Volcanic hazards at the proposed high-level radioactive waste repository at Yucca Mountain, Nevada, are related to the proximity of the site to Quaternary basaltic cinder cones. There is a possibility of volcanic activity at the site during $<10^4$ yr performance period of the proposed geologic repository at Yucca Mountain, the only site currently under consideration in the U.S. This proposed repository is expected to isolate approximately 70,000 to 100,000 metric tons of high-level radioactive waste from the biosphere. Consequently, accurate quantitative assessments of volcanic hazards at the site form an important component of the overall risk assessment for the repository.

The long-term hazards posed by formation of new basaltic volcanic vents is not unique to Yucca Mountain. Other sites where the opening of new vents at or near the nuclear facility is considered to be a potential volcanic hazard [*International Atomic Energy Agency*, 1997; *Code of Federal Regulations*, 1994] include the Mülheim-Kärlach nuclear power plant, Germany [*G. Wörner*, written communication to B.E. Hill, 1995]; the New Production Reactor, Idaho [*Volcanism Working Group*, 1990]; the proposed Muria, Indonesia, nuclear power plant; and the existing Medzamor nuclear power plant, near Yerevan, Armenia [*Connor et al.*, 1998a].

The first goal of this paper is to introduce a new method of quantifying the probability of formation of new volcanic vents at sites located within or near active volcanic fields. Particular emphasis is placed on the likely locations of future volcanic vents based on past patterns of volcanism and tectonism. The objective of this type of analysis is not to predict the future locations of cinder cones or other volcanic vents—an impossible task—but to provide a distribution function for likely vent locations based on current understanding of the processes controlling basaltic volcanism. The second goal is to use this method to estimate the probability of volcanic eruptions at the proposed Yucca Mountain repository. This analysis accounts for tectonic features of the Yucca Mountain region (YMR) that influence volcano distribution [*Connor et al.*, 1998b] and results in higher probability of volcanic eruptions at the site compared to previous hazard estimates [*Crowe et al.*, 1982; 1992; *Ho et al.*, 1991; *Connor and Hill*, 1995; *Geomatrix*, 1996].

Basaltic Volcanoes in the Yucca Mountain Region

Detailed accounts of the geology and geochronology of YMR basalts are found in *Byers et al.* [1966], *Carr and Quinlivan* [1966], *Byers and Barnes* [1967], *Byers and Cummings* [1967], *Hinrichs et al.* [1967], *Noble et al.* [1967], *Tschanz and Pampeyan* [1970], *Cornwall* [1972], *Vaniman et al.* [1981], *Crowe* [1990], *Crowe et al.* [1983, 1986], *Carr* [1984], *Swadley and Carr* [1987], *Faulds et al.* [1994], *Fleck et al.* [1996], and *Stamatakos et al.* [1997]. Geophysical data used to supplement geological data, especially where basaltic volcanoes are buried or partially buried by alluvial sediments, is presented in *Langenheim et al.* [1993], *Langenheim* [1995], *Stamatakos et al.* [1997], and *Connor et al.* [1997, 1998b]. Much of this work, including the map locations of basaltic volcanoes (Figure 1) and age distributions for these volcanoes, is summarized in *Connor and Hill* [1995].

Briefly, the YMR has been the site of recurring small volume basaltic volcanism since the Miocene. In the Pliocene and Quaternary, this basaltic volcanic activity focused in Crater Flat and the Amargosa Valley, west and south of the repository site. Much of the Quaternary volcanic activity in the YMR occurred approximately 1 Ma, during the formation of an alignment of five cinder cones in Crater Flat [*Bradshaw and Smith*, 1994; *Stamatakos et al.*, 1997]. Additional volcanism formed two cones about 30 km NW of Crater Flat, near Sleeping Butte, at approximately 0.3 Ma. The most recent volcanism in the YMR occurred at Lathrop Wells cinder cone, approximately 0.1 Ma [*Turrin et al.*, 1991; *Crowe et al.*, 1992]. This Quaternary volcanic activity occurred in close proximity to Pliocene volcanic centers, indicating that volcanism in these clusters is long lived and controlled by extension and extensional structures [*Connor et al.*, 1998b].

Definition of Volcanic Events

To assess a volcanic hazard, one may begin by formulating the null hypothesis: a volcanic event will occur at the site within the performance period of the facility. Analysis is then directed toward quantifying the confidence with which this null hypothesis may be rejected in favor of an alternate hypothesis—that a volcanic event will not occur during the performance period of the facility [*McBirney*, 1992].

In evaluating the null hypothesis, the definition of the volcanic event is a critical step, on which all subsequent estimates of recurrence rates and probability depend. For this analysis, an event is defined as an extrusive volcanic occurrence distinct and independent of other occurrences. An event is distinct from and independent of other events if the event is separated from other events in space, time, or both. Some flexibility is introduced by this definition because individual volcanic vents, or alignments of vents of similar ages, can be considered to be single events. In practice, the sensitivity of the results to this variation in event definition is explored as part of the hazard analysis.

For sites containing young cinder cones, spatter mounds, and maars, an individual edifice can be assumed to represent an individual volcanic event [*Connor and Hill*, 1995]. If older, eroded vents, buds [*Delaney and Gartner*, 1997], and dikes are present, such as in Pliocene Crater Flat (Figure 1), determination of volcanic events is more complicated and requires interpretation of these structures. In the YMR, ten additional volcanoes, completely buried by alluvium, have been discovered through interpretation of aeromagnetic and ground magnetic data [*Langenheim et al.*, 1993; *Langenheim*, 1995; *Connor et al.*, 1997]. These anomalies are included in a conservative hazard assessment, although it is possible some of the magnetic anomalies are not produced by basaltic rocks.

Estimating the Probability of a Volcanic Event

Using the previous definition of volcanic events, the probability of a volcanic eruption through the repository, given an eruption somewhere in the region, can be approximated:

$$P[\text{eruption through repository} \mid \text{eruption centered at } x,y] = \begin{cases} 1, \text{if } x,y \in A_e \\ 0, \text{otherwise} \end{cases} \tag{1}$$

where the effective area, A_e, is the area of the repository and the region around the repository within one vent-conduit radius of the repository boundary [*Geomatrix*, 1996]. A_e may also encompass dike segments associated with the vent.

Assume the occurrence of volcanic events in space and time can be represented by a nonuniform Poisson process (i.e., the probability of k events in time interval Δt and space interval Δx, Δy is given by):

$$P[N=k] = \frac{[\lambda(x,y,t)\Delta x \Delta y \Delta t]^k \exp[-\lambda(x,y,t)\Delta x \Delta y \Delta t]}{k!} \tag{2}$$

where N is the number of events and $\lambda(x,y,t)$ is the space time dependent recurrence rate. For simplicity, assume that $\lambda(x,y,t) = \lambda_t \lambda_r$ where λ_t is the number of events per unit time (i.e., the regional recurrence rate) and λ_r is the number of events per unit area (i.e., a factor that weights the regional recurrence rate by area). Equation (2) can be written as:

$$P[N=k] = \frac{[\lambda_t \lambda_r \Delta t \Delta x \Delta y]^k \exp[-\lambda_t \lambda_r \Delta t \Delta x \Delta y]}{k!} \tag{3}$$

putting $k = 0$:

$$P[N=0]=\exp[-\lambda_t\lambda_r\Delta t\Delta x\Delta y] \tag{4}$$

Therefore:

$$P\text{ [one or more events occur within }\Delta x,\Delta y,\Delta t]=1-\exp[-\lambda_t\lambda_r\Delta t\Delta x\Delta y] \tag{5}$$

Because of the small rate of occurrence of volcanic events, the probability of more than one event is quite small within most periods of interest and hence, equation (5) represents the probability of one event in Δt, Δx, Δy. Putting $\Delta t = 1$ yr gives the probability of an event occurring within one year in the area Δx, Δy.

Putting $\Delta t = 1$ yr, the annual probability of one (or more) volcanic eruptions within the site boundary is given by:

$$P\text{[volcanic eruptions within repository boundary]} = 1-\exp[-\lambda_t\lambda_r A_e] \tag{6}$$

where $A_e = \Delta x \times \Delta y$.

Patterns in volcanic activity in the YMR and in other volcanic fields indicate that alternative definitions of volcanic events are also reasonable. *Connor et al.* [1998b] discuss vent alignment development in the YMR, including the Quaternary Crater Flat alignment and Aeromagnetic Anomaly "A" (Figure 1). Because many vents are part of alignments that formed over a relatively brief period of time compared to the average recurrence rate of volcanism in the field, vents along alignments may be considered to constitute a single volcanic event. Effectively, defining aligned volcanoes of similar ages as single volcanic events reduces both the total number of volcanic events in the region and the regional recurrence rate [*Sheridan*, 1992; *Geomatrix*, 1996]. The character of the hazard analysis changes, however, because volcanic events now have length and orientation. *Geomatrix* [1996] gave the probability that an event centered on a given location will result in intersection of an igneous intrusion with the repository. This probability is suitable for the probability of vent alignments intersecting the repository and can be expressed as:

$$P_L\left[L \geq l_r,\ \varphi_1 \leq \Phi \leq \varphi_2\right] = \int_{l_r}^{\infty}\int_{\varphi_1}^{\varphi_2} f_L(l) \cdot f_\Phi(\varphi)\ d\varphi dl \qquad (7)$$

where Φ is the azimuth of the vent alignment, with φ_1 and φ_2 representing the range of azimuths that would result in intersection with the repository, given an igneous event centered on x, y—a distance l_r from the repository boundary. This expression assumes that φ_1, φ_2 are not functions of x, y, which appears reasonable based on shallow dike distributions [*Delaney and Gartner*, 1997]. The probability that the vent alignment length, L, will exceed l_r at an azimuth between φ_1 and φ_2 depends on the probability density functions $f_L(l)$ for alignment half-length and $f_\Phi(\varphi)$ for azimuth.

If volcanic events are defined as vents and vent alignments, the annual probability of an igneous event centered at x, y becomes:

$$P_{x,y} = 1 - \exp\left(-\lambda_t \lambda_r \Delta x \Delta y\right) \tag{8}$$

In practice, λ_r can be approximated on a grid of points with map extent X, Y and grid spacing Δx, Δy. The probability of volcanic eruptions disrupting the repository is then:

$$P[\text{volcanic eruption disrupting the respository in 1 yr}] = \sum_{i=1}^{X} \sum_{j=1}^{Y} P_{x,y}(x_i, y_j) \cdot P_L(x_i, y_j) \tag{9}$$

In the following sections, parameters related to the temporal recurrence rate of volcanism, spatial recurrence rate of volcanism, and length and orientation of vent alignments in the YMR are discussed and evaluated, then used to calculate probability of eruptions at the proposed repository using Equations (1)–(9).

Temporal Recurrence Rate, λ_t

Probability models rely on estimates of the expected regional recurrence rate of volcanism to calculate the probability of future volcanic activity. Previous estimates of λ_t for the YMR yielded estimates of expected regional recurrence rate between 2 and 12 volcanic events per million years (v/my) [e.g., *Ho*, 1991; *Ho et al.*, 1991; *Crowe et al.*, 1992, 1993; *Margulies et al.*, 1992; *Connor and Hill*, 1995], with various definitions of volcanic event and the extent of the volcanic field accounting for most of this range.

The simplest approach to estimate regional recurrence rate is to average the number of volcanic events that occurred during some time period of arbitrary duration. For instance, *Ho et al.* [1991] averaged the number of volcanoes formed during the Quaternary (1.6 m.y.) to calculate the recurrence rate. Through this approach they estimate an expected recurrence rate of 5 v/my. *Crowe et al.* [1982] averaged the number of new volcanoes over a 1.8 million-year period. *Crowe et al.* [1992] considered the two Little Cones (Figure 1) to represent a single volcanic event, and therefore concluded there are seven Quaternary volcanic events in the region. This lowers the estimated recurrence rate to approximately 4 v/my.

An alternative approach is the repose time method [*Ho et al.*, 1991], in which a regional recurrence rate is defined using a maximum likelihood estimator that averages events over a specific period of volcanic activity:

$$\lambda_t = \frac{(E-1)}{(T_o - T_y)} \tag{10}$$

where E is the number of events, T_o is the age of the first event, T_y is the age of the most recent event, and λ_t is the estimated regional recurrence rate. Using eight Quaternary volcanoes as the number of events, E, and 0.1 Ma for the formation of Lathrop Wells, the estimated recurrence rate depends on the age of the first Quaternary volcanic eruption in Crater Flat. Using Matuyama ages for Quaternary Crater Flat volcanism, 0.98 Ma $\leq T_o \leq$ 0.77 Ma [*Stamatakos et al.*, 1997], giving 8 v/my $\leq \lambda_t \leq$ 10 v/my. Grouping vent alignments formed during the Quaternary, $E = 3$ and the recurrence rate is 2–3 v/my. The repose time method has distinct advantages over techniques that average over an arbitrary period of time because it restricts the analysis to a time meaningful to volcanic activity. In this sense, it is similar to methods applied previously to estimate time-dependent relationships in active volcanic fields [*Kuntz et al.*, 1986]. *Ho* [1991, 1996] applied a Weibull-Poisson technique to estimate the recurrence rate of new volcano formation in the YMR as a function of time. Although this nonstationary approach is intriguing, it has been strongly criticized because it tends to impose monotonic trends on rates of volcanic activity [*Bebbington and Lai*, 1996] and because of the paucity of data available to construct nonstationary models for YMR volcanism [*Crowe and Perry*, 1989; *Crowe et al.*, 1993; *Connor and Hill*, 1993].

Spatial Weighting Factor, λ_r

Early models assessing the probability of future volcanism in the YMR and the likelihood of a repository-disrupting igneous event relied on the assumption that Plio-Quaternary basaltic volcanoes are distributed in a spatially uniform random manner over some bounded area [e.g., *Crowe et al.*, 1982, 1992; *Ho et al.*, 1991; *Margulies et al.*, 1992]. Patterns in the distribution and age of basaltic volcanoes in the YMR, however, make the choice of these bounded areas somewhat subjective. For example, *Smith et al.* [1990] and *Ho* [1992] define NNE-trending zones within which average recurrence rates exceed that of the surrounding region. These zones correspond to cinder cone alignment orientations that *Smith et al.* [1990] and *Ho* [1992] hypothesize may occur as a result of structural control. Employing such narrow zones leads to comparatively high estimates of spatial recurrence rate and probability of volcanic disruption of the proposed repository site. Conversely, using bounded areas that are large compared to the current distributions of cinder cone clusters results in relatively low estimates of spatial recurrence rate. *Ho* [1991] argued that under these circumstances, using narrow bounding areas, which include the proposed repository, give conservative estimates of probability of volcanic disruption.

Alternatively, spatial recurrence rate can be estimated using models that explicitly account for volcano clustering. Vent clustering results in 1–2 orders of magnitude change in estimates of spatial recurrence rate across the YMR [*Connor and Hill*, 1995; *Connor et al.*, 1998b] and this feature of vent distribution can be considered explicitly in the hazard analysis using kernel functions [*Silverman*, 1986; *Lutz and Gutmann*, 1995; *Connor and Hill*, 1995; *Condit and Connor*, 1996; *Conway et al.*, 1998]. A kernel is a function that assigns weights to the locations of future volcanic events, based on the positions of existing volcanic vents or related geologic data. Several types of kernels, including Gaussian and Epanechnikov, are discussed by *Silverman* [1986]. All multivariate kernels have the property:

$$\int_{\mathbf{R}} K(\mathbf{x})\ d\mathbf{x} = 1 \tag{11}$$

where K(**x**) is the kernel function and **x** is an *n*-dimensional vector. A Gaussian kernel is:

$$K(x,y) = \frac{1}{2\pi h^2}\exp\left\{-\frac{1}{2}\left[\left(\frac{x-x_v}{h}\right)^2 + \left(\frac{y-y_v}{h}\right)^2\right]\right\} \tag{12}$$

where the kernel is calculated at a point x,y and the center of the kernel, in this case the volcano location, is x_v, y_v . The kernel is normalized using the smoothing parameter, h, equivalent to the standard deviation of the distribution.

If x and y locations are on a rectangular grid, the spatial weighting function based on the distribution of N volcanoes is:

$$\lambda_r(x,y) = \frac{1}{N}\sum_{i=1}^{N} K(x,y;x_{v_i},y_{v_i}) \tag{13}$$

Equations (12) and (13) can be used to estimate the probability of volcanic eruptions at a site, given a vent-forming volcanic eruption in the region. The results of this probability estimate depend on h . One approach to bounding uncertainty in the resulting probability estimates is to evaluate probability using a wide range of h values [*Connor and Hill*, 1995]. Alternatively, the effectiveness of the kernel model and optimal values of h can be deduced from the distribution of nearest-neighbor distances between existing volcanoes. For example, the two-dimensional Gaussian kernel model can be compared with the distribution of nearest-neighbor distances between existing volcanoes by recasting the kernel function in polar coordinates, assuming that the weight is independent of θ:

$$K(r,\theta) = \frac{2}{h(2\pi)^{\frac{3}{2}}}\exp\left[-\frac{1}{2}\left(\frac{r^2}{h^2}\right)\right] \tag{14}$$

where r is distance from the volcanic event, x_v, y_v. The expected fraction of volcanic events within distance R of their nearest-neighbor volcanic event is then:

$$\hat{F}(R) = \int_0^{2\pi}\int_0^{R} \frac{2}{h(2\pi)^{\frac{3}{2}}} \exp\left[-\frac{1}{2}\left(\frac{r^2}{h^2}\right)\right] dr d\theta, \; R \geq r \tag{15}$$

Treating all vents as individual volcanic events, the distance between nearest-neighbor vents varies from ~200 m to 25 km. The mean distance to nearest-neighbor volcanic event is 3.8 km with a standard deviation of 5.8 km. Some vents such as SW and NE Little Cones are quite closely spaced (400 m) and have been treated as single volcanic events in some hazard analyses [*Crowe et al.*, 1992; *Connor and Hill*, 1995]. Treating vents spaced more closely than 1 km as single volcanic events, the mean distance to nearest-neighbor volcanic event increases to 5.0 km and the standard deviation increases to 5.9 km. Alternatively, defining volcanic events as vents and vent alignments gives a mean distance to nearest-neighbor volcanic event as 7.0 km, with a standard deviation of 6.4 km.

The observed distance to nearest-neighbor volcanic event in the YMR is shown cumulatively for each of these three definitions in Figure 2. These observed distributions are compared to expected distribution functions based on Equation (15) and $h = 3$–9 km. Comparison of expected and observed distribution leads to a natural definition of conservatism for a site-specific hazard analysis. For example, the distance between the proposed repository and its nearest-neighbor Quaternary volcano is 8.2 km. Gaussian kernel functions with $h = 7$–9 km are conservative because a greater fraction of volcanic events occurs at nearest-neighbor distances less than 8.2 km than predicted by the model. In contrast, the Gaussian kernel function with $h = 3$ km is not conservative because a smaller fraction of volcanic events occur at nearest-neighbor distances of 8.2 km than predicted by the model (Figure 2). In other words, probability models using $h = 7$–9 km are not likely to underestimate hazard for the YMR vent distribution. An $h = 5$ km smoothing parameter is conservative for probability models based on individual vent distributions; but not for a model based on vent alignment distributions.

The Epanechnikov kernel function is widely used to estimate spatial recurrence rate in basaltic volcanic fields [*Lutz and Gutmann*, 1995; *Connor and Hill*, 1995; *Condit and Connor*, 1996] and may be tested in a similar manner as the Gaussian kernel function. The Epanechnikov kernel in 2D Cartesian coordinates is:

$$K(x,y) = \frac{2}{\pi h^2}\left\{1 - \left[\left(\frac{x-x_v}{h}\right)^2 + \left(\frac{y-y_v}{h}\right)^2\right]\right\} \tag{16}$$

which integrates to unity provided that:

$$\sqrt{(x - x_v)^2 + (y - y_v)^2} \leq h \tag{17}$$

otherwise:

$$K(x,y) = 0 \tag{18}$$

In polar coordinates this kernel function becomes:

$$K(r,\theta) = \frac{3}{4\pi h}\left[1-\left(\frac{r^2}{h^2}\right)\right], \quad r \le h \tag{19}$$

The expected number of nearest-neighbor vents within distance r, is then:

$$\hat{F}(R) = \int_0^{2\pi}\int_0^{R}\frac{3}{4\pi h}\left[1 - \left(\frac{r^2}{h^2}\right)\right]dr d\theta, \; R \le h \tag{20}$$

As was accomplished for the Gaussian kernel, the cumulative probability density function for the Epanechnikov kernel can be compared with the observed fraction of volcanoes erupted at a given nearest-neighbor distance or less for various values of h (Figure 3). This comparison indicates that an Epanechnikov kernel function with $h = 10$ km best models the distribution of distance to nearest-neighbor volcanic event, if volcanic events are defined as vents or vent pairs. If volcanic events are defined as vents or vent alignments, 10 km $< h <$ 18 km better approximates the distribution of distances to nearest-neighbor volcanic events, given the current distribution of volcanoes.

Comparing the Epanechnikov and Gaussian kernel models indicates that the Gaussian kernel models better fit the observed distribution than Epanechnikov distributions, particularly at nearest-neighbor distances greater than 6 km. The difficulty fitting the observed distributions with the Epanechnikov kernel function results from truncation of this distribution at distances greater than h, which is unrealistic, particularly for analyses based on comparatively few events.

Furthermore, probability estimates can vary widely with *h* using the Epanechnikov kernel where the site is close to the edge of the volcanic field.

Vent alignment length and orientation

If the volcanic event consists of development of a vent or vent alignment, mapped vent locations are useful in constraining the functions $f_\Phi(\varphi)$ and $f_L(l)$ [equation (7)]. In the YMR Plio-Quaternary, six volcanic events resulted in the formation of isolated vents and four volcanic events resulted in the formation of vent alignments. Of these four vent alignments, the Pliocene Crater Flat vents and the Sleeping Butte vent pair are less than 4 km long. The Amargosa Desert Aeromagnetic Anomaly "A" alignment is slightly longer than 4 km. The Quaternary Crater Flat alignment, one of the youngest and most important volcanic events in the YMR, is also the longest alignment: approximately 11 km based on mapped vents, and 16 km long if ground magnetic anomalies are included [*Connor et al.*, 1998b]. Although these data provide an idea of the range of alignment lengths possible in the YMR, they are not sufficient to estimate a probability distribution for vent alignment lengths, $f_L(l)$.

Data from other volcanic fields can be useful in bounding $f_L(l)$. *Draper et al.* [1994] mention that approximately 30 percent of the vents in the San Francisco volcanic field form alignments and the remaining vents are isolated and appear to have formed during independent episodes of volcanic activity. This value appears to be comparable to the ratio of vent alignments to individual vents in the YMR. Data on vent alignment lengths from other volcanic fields suggests that vent alignments may be considerably longer than the Quaternary Crater Flat alignment. For example, *Connor et al.* [1992] identified vent alignments > 20 km in length in the Springerville volcanic field, Arizona. Vent alignments of comparable or greater length were also identified in the Michoacan-Guanajuato volcanic field, Mexico [*Wadge and Cross*, 1988; *Connor*, 1990], and the Pinacate volcanic field, Mexico [*Lutz and Gutmann*, 1995]. Based on mapping in the Lunar Crater, Reveille Range, and San Francisco volcanic fields, *Smith et al.* [1990] suggested that alignments may be up to 20 km-long, with a lower probability of 40 km long alignments. None of these authors, however, developed distributions for vent alignment lengths in these areas. Furthermore, it is not clear whether the conditions for vent alignment formation and factors controlling vent alignment lengths are comparable between these different regions and the YMR [*Connor et al.*, 1998b], and vent alignments can remain episodically active for long periods of time [*Conway et al.*, 1997].

Given the caveat that data about $f_L(l)$ are scarce, the probability density function for event length can be expressed as:

$$f_L(l) = \begin{cases} \frac{1}{2}, \ l = 0 \\ \frac{U[l_{min}, l_{max}]}{2}, \ l > 0 \end{cases} \tag{21}$$

By this definition, there is 50 percent probability that igneous events do not form vent alignments and only disrupt the repository if they fall within the effective area, A_e, of the site. The remaining igneous events form alignments that affect areas up to a distance l_{max} from the point x, y. This percentage assigned to zero-length igneous events is a source of uncertainty in probability estimates and is not well constrained by available data. The probability density function is construed to be a uniform random distribution between l_{min} and l_{max} because the distribution of alignment lengths is also poorly known.

Using this definition of $f_L(l)$, probability estimates of intersection of the repository, given an event at x, y, will not be strongly dependent on l_{min} compared to l_{max}. The value of l_{max} can be chosen as 5.5–8 km, taking the Quaternary Crater Flat alignment as the maximum alignment half-length. Given observations in other volcanic fields, however, l_{max} may be 10 km or more.

The distribution function for alignments or dike zone azimuth, $f_\Phi(\varphi)$, is better constrained by the data on vent alignments, regional stress distribution, and the orientations of high-dilation tendency faults. Three of the alignments in the YMR trend 020°–030°, perpendicular to the least principal horizontal compressional stress in the region, approximately 028° [e.g., *Morris et al.*, 1996]. Under these circumstances, $f_\Phi(\varphi)$ may vary over a narrow range. For example,

$$f_\Phi(\varphi) = U[020°, 035°] \tag{22}$$

Probability Calculations

The spatial weighting factor is estimated from the kernel function, smoothing parameter, and number of volcanic events [equation (13)]. For the following calculations, the spatial weighting factor is estimated on a grid, where Δx and Δy = 1000 m; x,y is 548,500 m East; 4,078,500 m North; and x_v, y_v are in Universal Transverse Mercator, *North American Datum*, 1983, coordinates. Smoothing parameters, $h \geq 5$ km, are appropriate for the Gaussian kernel. An effective repository area of 5.49 km^2 is used in this analysis, based on the current repository design and a 50-m buffer zone about the repository perimeter. The number of volcanic events, *N*, depends on whether Pliocene and Quaternary or only Quaternary volcanoes are considered in the probability estimate and in the definition of a volcanic event—both influence λ_t . For the following calculations, 2 v/my $\leq \lambda_t \leq$ 12 v/my.

Based on these estimates of λ_r, λ_t, and A_e, the annual probability of volcanic eruptions within the repository boundary is between 0.5×10^{-8} and 3.5×10^{-8} [equation (6), Figure 4]. Probabilities are slightly higher if the distribution of Quaternary volcanoes is considered in estimation of $\lambda_r(x,y)$ rather than the distribution of Plio-Quaternary volcanoes, because Quaternary volcanoes are, on average, located nearer to the repository site. These values are quite close to those calculated by *Connor and Hill* [1995] using Epanechnikov kernel and nearest-neighbor estimators of spatial and spatio-temporal recurrence rate. *Connor and Hill* [1995] used $A_e = 8$ km^2 and estimated annual probabilities of volcanic disruption of the site between 1×10^{-8} and 5×10^{-8}.

These estimates change slightly when vent alignments are included in the definition of volcanic events. Annual probability of volcanic eruptions within the repository boundary was calculated using $l_{min} = 100$ m; 5,200 m $\leq l_{max} \leq$ 10,200 m; and 5 km $\leq h \leq$ 7 km [Equations (7)–(9), Figure 5]. Using the three Quaternary igneous events, Lathrop Wells, Quaternary Crater Flat, and the Sleeping Butte alignment, annual probabilities of volcanic eruptions within the repository boundary range between 1×10^{-8} and 4×10^{-8}, assuming a regional recurrence rate of 3 v/my. Using a recurrence rate of 5 v/my results in annual probabilities of up to 6×10^{-8}.

The standard Gaussian kernel model presented here may be modified to incorporate variation in crustal density by developing a weighting function that takes crustal density into account. The model for basaltic volcanism in extensional environments developed in *Connor et al.* [1998b] relates pressure gradients in the lithospheric mantle to regional changes in crustal density caused by extension. Pressure gradients in the lithospheric mantle however, are likely transitory and small, thus only mantle rocks already close to their solidus will partially melt as a result of extension—a factor that may strongly influence basaltic volcano clustering.

Direct evidence of pressure change in the mantle can only be inferred conceptually with the assistance of simple numerical models of mantle stresses [*Connor et al.*, 1998b]. The weighting function can be estimated from the frequency of volcanic eruptions as a function of crustal density. The distribution of this function, $f_T(x,y)$, is defined based on average crustal densities in the upper 5 km of the crust at the locations of existing volcanoes (Figure 6). The Gaussian kernel is then modified to estimate the recurrence rate of volcanism at x, y:

$$Q_v = \frac{\sum_{i=1}^{X}\sum_{j=1}^{Y} K(x_i,y_j)}{\sum_{i=1}^{X}\sum_{j=1}^{Y} f_T(x_i,y_j) \cdot K(x_i,y_j)} \qquad (23)$$

$$\lambda_r(x,y) = \frac{1}{N} \sum_{v=1}^{N} Q_v \, f_T(x_i,y_j) \; K_g(x_i,y_j) \tag{24}$$

Introduction of the ratio Q_v assures that the integral of the modified Gaussian kernel for a single volcano over a large map extent X, Y relative to the smoothing parameter, h, will be unity [equation (11)]. Probability will be redistributed based on crustal density variations in the vicinity of the volcano.

Comparison of the modified and standard kernels is made by contouring $\lambda_r(x,y)$ across the YMR, using the distribution of Quaternary vents, vent alignments, and $h = 9$ km. As previously noted, $N = 3$ in this model, including Quaternary Crater Flat, Lathrop Wells, and Sleeping Butte as the three Quaternary volcanic events. In Figure 7, $\lambda_r(x,y)$ is contoured across the map region using equation (13). Given an igneous event in the region, there is approximately 68 percent chance it will occur within this map area. The Sleeping Butte alignment NNW of the mapped region accounts for the remaining probability (Figure 1). Larger values of the spatial weighting factor, $\lambda_r(x,y)$, indicate areas where igneous events are most likely to be centered. The largest values occur in southern Crater Flat because of the proximity of Lathrop Wells and the Quaternary Crater Flat alignment.

Figure 8 is based on the modified kernel [equations (23)–(24)] using the same parameters as used in the standard kernel calculation ($N = 3$, $h = 9$ km), but weighting the kernel using crustal densities variations. Use of the modified kernel reduces the area of the $\lambda_r(x,y)$ surface at, for example, the 2×10^{-4} v/km^2 contour and increases the amplitude of the surface. The $\lambda_r(x,y)$ surface also becomes asymmetric when applying the modified kernel function. Values of $\lambda_r(x,y)$ are greatest in southern Crater Flat, exceeding 1.2×10^{-3} v/km^2, and decrease abruptly near the Bare Mountain fault. Probability values decrease less abruptly on the eastern boundary of Crater Flat because crustal densities change less rapidly on the eastern edge of the basin. This more gradual change in $\lambda_r(x,y)$ on the eastern edge of the basin is consistent with the proposed model linking crustal extension and basaltic volcanism [*Connor et al.*, 1998b].

The estimated annual probability of volcanic eruptions within the repository boundary increases when the modified kernel function is used. Annual probability of volcanic eruptions within the repository boundary were calculated using 5,200 m $\leq l_{max} \leq$ 10,200 m, and h = 7 km. Using the three Quaternary igneous events, Lathrop Wells, Quaternary Crater Flat, and the Sleeping Butte alignment results in annual probabilities of volcanic eruptions within the repository boundary between 3×10^{-8} and 5.5×10^{-8}, assuming a regional recurrence rate of 3 v/my (Figure 9).

Including Pliocene volcanoes in the estimation of $\lambda_r(x,y)$ decreases the annual probability at the repository because many Pliocene volcanoes are located in the Amargosa Desert. Annual probabilities based on the modified kernel distribution and Plio-Quaternary volcanoes vary between 1.5 and 3×10^{-8}, comparable to the annual probabilities estimated using the standard kernel and the distribution of Quaternary vents and vent alignments.

The regional recurrence rate of vent and vent alignment formation is poorly constrained in the YMR. Varying regional recurrence rate of volcanic events between 1 and 5 v/my results in nearly one order of magnitude variation in the annual probability of volcanic eruptions within the repository boundary. Using the modified kernel model, $h = 7$ km and 5,200 m $\leq l_{max} \leq$ 10,200 m, annual probability of volcanic eruptions within the repository varies between 1×10^{-8} and 9×10^{-8} (Figure 10).

Discussion

Annual probability of volcanic eruptions within the proposed Yucca Mountain repository boundary vary between 1×10^{-8} and 1×10^{-7} based on a range of models. This range accounts for varying definitions of volcanic events and uncertainty in parameter distributions used to estimate probability. Annual probabilities are generally between 1×10^{-8} and 3×10^{-8} for volcanic events defined as individual mappable units and vents. This definition of volcanic events requires the fewest assumptions about underlying parameter distributions but also neglects some features of vent distribution important in the YMR. In particular, the formation of vent alignments is not considered in this model.

Defining volcanic events as vents and vent alignments results in a similar range of probability estimates: 1×10^{-8} to 6×10^{-8}. Although recurrence rates are lower using this definition of volcanic events, the area affected by individual events is greater. The distribution of alignment length and regional recurrence rate of these volcanic events introduces the greatest uncertainties into these probability models. Incorporating regional crust density variation into this model results in a model more closely linked to geologic processes, as elucidated by comparison of the Gaussian kernel and modified Gaussian kernel models (Figures 7 and 8). Based on the modified kernel models, the annual probability of volcanic eruptions within the repository boundary is between 1×10^{-8} and 9×10^{-8}.

This overall range of probability values, 1×10^{-8} to 1×10^{-7}, arises from the application of a variety of models and a range of parameter distributions. Nothing in the prior analysis suggests that this range of probabilities has central tendency, that the mean or median of this range of probabilities is significant, or that high or low values in this range are more or less likely. At least at the current time, it is not feasible to assign likelihood to the precision and accuracy of these models in a meaningful way. Thus the probability estimate is good to one order of magnitude and 10^{-7}/yr (10^{-3} for the 10^4 performance period of the facility), represents a reasonably conservative hazard estimate. By the same token, these parameter distributions and the resulting probability calculations do not reflect the full range of uncertainties in volcanic hazard estimates because new information can change these parameter distributions. For example, *Wernicke et al.* [1998] speculated that regional recurrence rate, λ_t, may be one order of magnitude greater than previously thought, based on anomalous GPS-derived crustal strain rates they observed in the YMR. If true, this change in regional recurrence rate would increase the upper bound of the hazard estimate to approximately 10^{-6}/yr, or 10^{-2} for the 10^4 performance period. Although the magnitude of these GPS strain rates [*Savage*, 1998] and their interpretation of hazard rates are debated [*Connor et al.*, 1998c], such data illustrate how hazard rates can be affected by evolving understanding of the geology of the volcanic systems.

It is worthwhile to assess this 10^{-7}/yr value in light of regional patterns of volcanism. The western Great Basin, which includes the YMR, comprises at least 211 basaltic volcanoes < 2 Ma within an 82,000 km^2 region [*Luedke and Smith*, 1981]. Simply averaging activity across the western Great Basin during the last 2 Ma yields a recurrence rate of 1.3×10^{-9} yr^{-1} km^{-2}. On average, the annual probability of volcanism within any 5 km^2 area (i.e., the effective area of the repository) is 6×10^{-9}. But volcanism strongly clusters in the western Great Basin. Yucca Mountain is part of one of the youngest of these volcano clusters and lies in an area of active crustal extension. Therefore, reasonably conservative estimates for the probability of volcanic eruptions at the proposed Yucca Mountain site should exceed this average regional estimate. In this respect, probability estimates as low as 10^{-10}/yr [*Geomatrix*, 1996; *Department of Energy*, 1998] are unrealistic.

Similarly, the probability of volcanism at the Yucca Mountain site can be compared to the most active basaltic volcanic fields in the continental United States. For example, recurrence rates in the Cima volcanic field, California, are on the order of 30 v/my [*Turrin et al.*, 1985]. On the Colorado Plateau, some volcanic fields experience similar recurrence rates [*Conway et al.*, 1998; *Condit and Connor*, 1996]. The probability of a volcanic event centered within a 5 km^2 area in one of these areas is on the order of 10^{-6}/yr–10^{-5}/yr. Comparable rates of basaltic volcanism have not occurred during the Plio-Quaternary in the YMR, with the possible exception of 4–5 Ma activity in the Funeral Formation of the southern YMR [*Conway et al.*, 1996]. It is reasonable that the probability estimates we calculate for volcanic eruptions at Yucca Mountain be substantially less than those estimated for these larger, more active volcanic fields.

Finally it should be noted that the relatively small annual probability of volcanic eruptions at the Yucca Mountain site, 10^{-7}/yr, must be viewed in light of the long performance period of the proposed repository. Although remanded, the *Code of Federal Regulations* [1994] for siting a high-level radioactive waste repository indicates that the effects of disruptive scenarios must be considered if their probability exceeds 10^{-4} in 10^{4} yr. Thus, a probability of 10^{-3} for the planned 10^{4} yr performance period of the repository is sufficiently great that the proximity of the site to this volcanic field must be considered in evaluations of the performance of a geologic repository. The ultimate assessment of suitability of the Yucca Mountain site will likely be based on risk to a reference group of individuals [*International Atomic Energy Agency*, 1986] located some distance away from the proposed site [*National Research Council*, 1995]. The effects of a volcanic eruption on repository performance and the risks associated with volcanism to this critical group need to be considered explicitly in evaluating suitability and expected performance of the Yucca Mountain site.

Acknowledgments

The authors thank Michael Conway and Wes Patrick for their technical reviews, Barbara Long for her editorial review, and Annette Mandujano for assistance preparing the manuscript. This paper was prepared as a result of work performed at the Center for Nuclear Waste Regulatory Analyses (CNWRA) for the U.S. Nuclear Regulatory Commission (NRC) under contract NRC-02-97-009. This paper is an independent product of the CNWRA and does not necessarily reflect the views or regulatory position of the NRC.

References

Bebbington, M.S., and C.D. Lai, On nonhomogenous models for volcanic eruptions, *Mathematical Geology, 28*, 585–600, 1996.

Bradshaw, T.K., and E.I. Smith, Polygenetic Quaternary volcanism at Crater Flat, Nevada. *J. Volcanol. Geotherm. Res., 63*, 165–182, 1994.

Byers, F.M., and H. Barnes, Geologic Map of the Paiute Ridge Quadrangle, Nye County, Nevada, *U.S. Geological Survey Geological Quadrangle Map GQ–577*, U.S. Geological Survey, Reston, VA, 1967.

Byers, F.M., and D. Cummings, Geologic Map of the Scrugham Peak Quadrangle, Nye County, Nevada, *U.S. Geological Survey Geological Quadrangle Map GQ–695*, U.S. Geological Survey, Reston, VA, 1967.

Byers, F.M., C.L. Rogers, W.J. Carr, and S.J. Luft, Geologic Map of the Buckboard Mesa Quadrangle, Nye County, Nevada, *U.S. Geological Survey Geological Quadrangle Map GQ–552*, U.S. Geological Survey, Reston, VA, 1966.

Carr, W.J., Regional and structural setting of Yucca Mountain, southwestern Nevada, and Late Cenozoic rates of tectonic activity in part of the southwestern Great Basin, Nevada and California, *USGS Open-File Report 84–854*, U.S. Geological Survey, Reston, VA, 1984.

Carr, W.J., and W.D. Quinlivan, Geologic Map of the Timber Mountain Quadrangle, Nye County, Nevada, *U.S. Geological Survey Geological Quadrangle Map GQ–503*, U.S. Geological Survey, Reston, VA, 1966.

Code of Federal Regulations, *Title 10, Part 60.122*, Code of Federal Regulations, Title 10, Parts 51–199, Washington, D.C., Office of the Federal Register, National Archives and Records Administration, 612 p., 1994.

Condit, C.D., and C.B. Connor, Recurrence rates of volcanism in basaltic volcanic fields: An example from the Springerville volcanic field, Arizona, *Geol. Soc. Am. Bull., 108*, 1,225–1,241, 1996.

Connor, C.B., Cinder cone clustering in the TransMexican volcanic belt: Structural and petrologic implications, *J. Geophys. Res., 95*, 19,395–19,405, 1990.

Connor, C.B., and B.E. Hill, Three nonhomogeneous Poisson models for the probability of basaltic volcanism: Application to the Yucca Mountain region, Nevada, U.S.A., *J. Geophys. Res., 100(B6)*, 10,107–10,125, 1995.

Connor, C.B., and B.E. Hill, Estimating the probability of volcanic disruption of the candidate Yucca Mountain repository using spatially and temporally nonhomogeneous Poisson models, in *Proceedings of the American Nuclear Society Focus '93 Meeting*, pp. 174–181, American Nuclear Society, La Grange Park, IL, 1993.

Connor, C.B., A.R. Godoy, and B.E. Hill, Long-term volcanic hazard assessment for nuclear facilities: Examples from the USA, Armenia, and Indonesia, invited paper presented at *Colima Volcano Sixth International Meeting*, Universidad de Colima, Colima, Mexico, January 26–30, 1998a.

Connor, C.B., J.A. Stamatakos, D.A. Ferrill, B.E. Hill, G. Ofoegbu, and F.M. Conway, Volcanic hazards at the proposed Yucca Mountain, Nevada, high-level radioactive waste repository I: Geologic factors controlling patterns of small-volume basaltic volcanism, *submitted*, 1998b.

Connor, C.B., J.A. Stamatakos, D.A. Ferrill, and B.E. Hill, Technical comment on: Anomalous strain accumulation in the Yucca Mountain area, Nevada, *Science*, in press, 1998c.

Connor, C.B., S. Lane-Magsino, J.A. Stamatakos, R.H. Martin, P.C. La Femina, B.E. Hill, and S. Lieber, Magnetic surveys help reassess volcanic hazards at Yucca Mountain, Nevada, *EOS, Trans. AGU, 78(7)*, 73–78, 1997.

Connor, C.B., C.D. Condit, L.S. Crumpler, and J.C. Aubele, Evidence of regional structural controls on vent distribution: Springerville volcanic field, Arizona, *J. Geophys. Res. 97*, 12,349–12,359, 1992.

Conway, F.M., C.B. Connor, B.E. Hill, C.D. Condit, K. Mullaney, and C.M. Hall, Recurrence rates of basaltic volcanism in SP cluster, San Francisco volcanic field, Arizona, *Geology, in press*, 1998.

Conway, M.F., D.A. Ferrill, C.M. Hall, A.P. Morris, J.A. Stamatakos, C.B. Connor, A.N. Halliday, and C. Condit, Timing of basaltic volcanism along the Mesa Butte Fault in the San Francisco volcanic field, Arizona, from 40Ar/39Ar dates: Implications for longevity of cinder cone alignments, *J. Geophys. Res., 102*, 815–824, 1997.

Conway, F.M., C.B. Connor, B.E. Hill, and D.A. Ferrill, Landsat TM, SPOT, and SLAR interpretation of volcanic and structural features of the Greenwater and Saline ranges, Inyo County, California, USA, *EOS, Trans. AGU, 77*, F793, 1996.

Cornwall, H.R., Geology and mineral deposits of southern Nye County, Nevada, *NV Bur. Mines Geo. Bull., 77*, 1972.

Crowe, B.M., Basaltic volcanic episodes of the Yucca Mountain region, in *Proceedings of the International Topical Meeting High-Level Radioactive Waste Management*, pp. 65–73, American Nuclear Society, La Grange Park, IL, 1990.

Crowe, B.M., and F.V. Perry, Volcanic probability calculations for the Yucca Mountain site: Estimation of volcanic rates, in *Proceedings of the Topical Meeting on Nuclear Waste Isolation in the Unsaturated Zone, FOCUS '89*, pp. 326–334, American Nuclear Society, La Grange Park, IL, 1989.

Crowe, B.M., F.V. Perry, G.A. Valentine, P.C. Wallmann, and R. Kossik, Simulation modeling of the probability of magmatic disruption of the potential Yucca Mountain site, in *Proceedings of the Topical Meeting on Site Characterization and Model Validation, FOCUS '93*, pp. 182–191, American Nuclear Society, La Grange Park, IL, 1993.

Crowe, B.M., R. Picard, G. Valentine, and F.V. Perry, Recurrence models for volcanic events: Applications to volcanic risk assessment, from *Third Conference on Radioactive Waste Management*, pp. 2,344–2,355, American Nuclear Society, La Grange Park, IL, 1992.

Crowe, B.M., K.H. Wohletz, D.T. Vaniman, E. Gladney, and N. Bower, Status of volcanic hazard studies for the Nevada Nuclear Waste Storage Investigations, Vol. II, LA–9325–MS, Los Alamos National Laboratory, Los Alamos, NM, 1986.

Crowe, B.M., D.T. Vaniman, and W.J. Carr, Status of volcanic hazard studies for the Nevada Nuclear Waste Storage Investigations, LA–9325–MS, Los Alamos National Laboratory, Los Alamos, NM, 1983.

Crowe, B.M., M.E. Johnson, and R.J. Beckman, Calculation of the probability of volcanic disruption of a high-level nuclear waste repository within southern Nevada, USA, *Radioactive Waste Management and the Nuclear Fuel Cycle, 3*, 167–190, 1982.

Delaney P.T., and A.E. Gartner, Physical processes of shallow dike emplacement near the San Rafael Swell, Utah, *Geol. Soc. Am. Bull, 109*, 1,177–1,192, 1997.

Draper, G., Z. Chen, M. Conway, C.B. Connor, and C.D. Condit, Structural control on magma pathways in the upper crust: Insights from the San Francisco volcanic field, Arizona, *Geol. Soc. Am. Abstr. Prog.*, A-115, 1994.

Faulds, J.E., J.W. Bell, D.L. Feuerbach, and A.R. Ramelli, Geologic Map of the Crater Flat Area, Nevada, *Nevada Bureau of Mines and Geology Map 101*, Nevada Bureau of Mines and Geology, Reno, NV, 1994.

Fleck, R.J., B.D. Turrin, D.A. Sawyer, R.G. Warren, D.E. Champion, M.R. Hudson, and S.A. Minor, Age and character of basaltic rocks of the Yucca Mountain region, southern Nevada, *J. Geophys. Res., 100(B4)*, 8,205–8,227, 1996.

Frizzell, V.A., Jr., and J. Shulters, Geologic Map of the Nevada Test Site, Southern Nevada, *Miscellaneous Investigations Map I–2046*, U.S. Geological Survey, Reston, VA, 1990.

Geomatrix, Probabilistic volcanic hazard analysis for Yucca Mountain, Nevada, *BA0000000–1717–2200–00082*, Geomatrix Consultants, San Francisco, 1996.

Hinrichs, E.N., R.D. Krushensky, and S.J. Luft, Geologic Map of the Ammonia Tanks Quadrangle, Nye County, Nevada, *U.S. Geological Survey Geological Quadrangle Map GQ–638*, U.S. Geological Survey, Reston, VA, 1967.

Ho, C.-H., Volcanic time-trend analysis, *J. Volcanol. Geotherm. Res.*, *74*, 171–177, 1996.

Ho, C.-H., Risk assessment for the Yucca Mountain high-level nuclear waste repository site: Estimation of volcanic disruption, *Math. Geol.*, *24*, 347–364, 1992.

Ho, C.-H., Time trend analysis of basaltic volcanism at the Yucca Mountain site, *J. Volcanol. Geotherm. Res.*, *46*, 61–72. 1991.

Ho, C.-H., E.I. Smith, D.L. Feurbach, and T.R. Naumann, Eruptive probability calculation for the Yucca Mountain site, USA: Statistical estimation of recurrence rates, *Bull. Volcanol.*, *54*, 50–56, 1991.

International Atomic Energy Agency, Principles for limiting releases of radioactive effluents into the environment, *Safety Series No. 77*, 32 pp., International Atomic Energy Agency, Vienna, Austria, 1986.

International Atomic Energy Agency, Volcanoes and associated topics in relation to nuclear power plant siting, *Provisional Safety Standards Series No. 1*, 49 pp., International Atomic Energy Agency, Vienna, Austria, 1997.

Jolly, R.J.H., and D.L. Sanderson, A Mohr circle construction for the opening of a pre-existing fracture, *J. Struct. Geol., 19*, 887–892, 1997.

Kuntz, M.A., D.E. Champion, E.C. Spiker, and R.H. Lefebre, Contrasting magma types and steady-state, volume-predictable, basaltic volcanism along the Great Rift, Idaho, *Geol. Soc. Am. Bull., 97*, 579–594, 1986.

Langenheim, V.E., *Magnetic and Gravity Studies of Buried Volcanic Centers in the Amargosa Desert and Crater Flat, Southwest Nevada*, USGS Open-File Report 95–564, U.S. Geological Survey, Reston, VA, 1995.

Langenheim, V.E., K.S. Kirchoff-Stein, and H.W. Oliver, Geophysical investigations of buried volcanic centers near Yucca Mountain, southwestern Nevada, *Proceedings of the Fourth*

Annual International Conference on High-Level Radioactive Waste Management, pp. 1,840–1,846, American Nuclear Society, La Grange Park, IL, 1993.

Luedke, R.G., and R.L. Smith, Map Showing Distribution, Composition, and Age of Late Cenozoic Volcanic Centers in California and Nevada, *U.S. Geological Survey Miscellaneous Investigations Series Map I–1091–C*, U.S. Geological Survey, Reston, VA, 1981.

Lutz, T.M. and J.T. Gutmann, An improved method for determining alignments of pointlike features and its implications for the Pinacate volcanic field, Mexico, *J. Geophys. Res.*, *100*, 17,659–17,670, 1995.

Margulies, T., L. Lancaster, N. Eisenberg, and L. Abramson, Probabilistic analysis of magma scenarios for assessing geologic waste repository performance, *92–WA/SAF–11*, American Society of Mechanical Engineers, New York, 1992.

McBirney, A.R., Volcanology, in *Techniques for Determining Probabilities of Geologic Events and Processes*, edited by R.L. Hunter and C.J. Mann, pp. 167–184, International Association for Mathematical Geology, Studies in Mathematical Geology No. 4, Oxford University Press, New York, 1992.

Minor, S.A, D.A. Sawyer, R.R. Wahl, V.A. Frizzell, Jr., S.P Schilling, R.G. Warren, P.P. Orkild, J.A. Coe, M.R. Hudson, R.J. Fleck, M.A. Lanphere, W.C. Swadley, and J.C. Cole, Preliminary Geologic Map of the Pahute Mesa 30' × 60' Quadrangle, Nevada, *U.S. Geological Survey Open-File Report 93–299*, U.S. Geological Survey, Reston, VA, 1993.

Morris, A., D.A., Ferrill, and D.B. Henderson, Slip-tendency analysis and fault reactivation, *Geology*, 24(3), 275–278, 1996.

National Research Council, *Technical Bases for Yucca Mountain Standards*, 205 pp. National Academy Press, Washington, DC, 1995.

Noble, D.C., R.D. Krushensky, E.J. McKay, and J.R. Ege, Geologic Map of the Dead Horse Flat Quadrangle, Nye County, Nevada, *U.S. Geological Survey Geological Quadrangle Map GQ–614*, U.S. Geological Survey, Reston, VA, 1967.

Savage, J.C., Technical comment on: Anomalous strain accumulation in the Yucca Mountain area, Nevada, *Science*, in press, 1998.

Sheridan, M.F., A Monte Carlo technique to estimate the probability of volcanic dikes, in *High Level Radioactive Waste Management, Proceedings of the Third International Conference*, pp. 2,033–2,038, American Nuclear Society, 2, La Grange Park, IL, 1992.

Silverman, B.W., *Density Estimation for Statistics and Data Analysis*, 175 pp., Chapman and Hall, London, 1986.

Smith, E.I., T.R. Feuerbach, and J.E. Faulds, The area of most recent volcanism near Yucca Mountain, Nevada: Implications for volcanic risk assessment, High-level Radioactive Waste Meeting, Proceedings of the International Topical Meeting, LaGrange Park, IL, *American Nuclear Society, 1*, 81–90, 1990.

Stamatakos, J.A., C.B. Connor, and R.H. Martin, Quaternary basin evolution and basaltic volcanism of Crater Flat, Nevada, from detailed ground magnetic surveys of the Little Cones, *J. Geol., 105*, 319–330, 1997.

Swadley, W.C., and W.J. Carr, Geologic Map of the Quaternary and Tertiary Deposits of the Big Dune Quadrangle, Nye County, Nevada, and Inyo County, California, *U.S. Geological Survey Miscellaneous Investigations Series Map I–1767*, U.S. Geological Survey, Reston, VA, 1987.

Tschanz, C.M., and E.H. Pampeyan, Geology and Mineral Deposits of Lincoln County, Nevada, *NV Bur. Mines Geol. Bull. 73*, 1970.

Turrin, B.D., D. Champion, and R.J. Fleck, $^{40}Ar/^{39}Ar$ age of the Lathrop Wells volcanic center, Yucca Mountain, Nevada, *Science, 253*, 654–657, 1991.

Turrin, B.D., J.C. Dohrenwend, R.E. Drake, and G.H. Curtis, K-Ar ages from the Cima volcanic field, eastern Mojave Desert, California, *Isochron West, 44*, 9–16, 1985.

U.S. Department of Energy, Repository safety strategy: U.S. Department of Energy's strategy to protect public health and safety after closure of a Yucca Mountain repository, YMP/96–01, 27 pp., U.S. Department of Energy, Office of Civilian Radioactive Waste Management, Washington, DC, 1998.

Vaniman, D.T., and B.M. Crowe, Geology and petrology of the basalts of Crater Flat: Applications to volcanic risk assessment for the nuclear waste storage investigations, *LA–8845–MS*, Los Alamos National Laboratory, Los Alamos, NM, 1981.

Vaniman, D.T., B.M. Crowe, and E.S. Gladney, Petrology and geochemistry of Hawaiite lavas from Crater Flat, Nevada, *Contributions in Mineralogy and Petrology, 80*, 341–357, 1982.

Volcanism Working Group, Assessment of potential volcanic hazards for new production reactor site at the Idaho National Engineering Laboratory, *UCRL–ID–104722*, 98 pp., Lawrence Livermore National Laboratory, Livermore, CA, 1990.

Wadge, G., and A. Cross, Quantitative methods for detecting aligned points: An application to the vents of the Michoacán-Guanajuato volcanic field, Mexico, *Geology, 16*, 815–818, 1988.

Wernicke, B., J.L. Davis, R.A. Bennett, P. Elósegui, M.J. Abolins, R.J. Brady, M.A. House, N.A. Niemi, and J.K. Snow, Anomalous strain accumulation in the Yucca Mountain area, Nevada, *Science, 279*, 2,096–2,100, 1998.

Figure Captions

Figure 1. Location map showing the proposed Yucca Mountain repository (double hachured lines), mapped Quaternary basaltic volcanoes (black), mapped Pliocene volcanoes and magnetic anomalies inferred to be buried volcanic features (gray), and Miocene basaltic volcanoes (hachured). Miocene caldera boundaries are shown as dashed lines and topography is contoured at 200 m intervals. Modified from *Frizzell and Schulters* [1990] and *Minor et al.* [1993]. Map projection is Universal Transverse Mercator, North American Datum, 1927; Zone 11.

Figure 2. Comparison of observed fraction of volcanoes within a given distance of their nearest-neighbor volcano with Gaussian kernel models calculated using h = 3 km, 5 km, 7 km, and 9 km. Observed curves include all vent (open squares), all vents or vent pairs more closely spaced then 1 km (solid circles), and vents and vent alignments (open circles). Buckboard Mesa (BB) is an outlier in the distribution as it is approximately 25 km from its nearest neighbor. The center of the repository site is located 8.2 km from Northern Cone, the nearest Quaternary volcano.

Figure 3. Comparison of observed fraction of volcanoes within a given distance of their nearest-neighbor volcano with Epanechnikov kernel models calculated using h = 5 km, 10 km, and 18 km. Observed curves include all vent (open squares), all vents or vent pairs more closely spaced then 1 km (solid circles), and vents and vent alignments (open circles). Buckboard Mesa (BB) is an outlier in the distribution as it is approximately 25 km from its nearest neighbor. The center of the repository site is located 8.2 km from Northern Cone, the nearest Quaternary volcano.

Figure 4. Annual probability of volcanic eruptions within the repository boundary. Events are defined as the formation of new vents. Gaussian kernel is used with smoothing parameter, *h*, varying from 0 to 20 km. Analysis of existing vent distribution indicates $h \geq$ 5km is suitable for volcanic hazard analysis at the repository. Curves are shown for various regional recurrence rates of volcanic vent formation ($\lambda_t = 2 \times 10^{-6}$ v/yr, 8×10^{-6} v/yr, 12×10^{-6} v/yr), based on the distribution of Quaternary volcanoes (heavy lines) and Plio-Quaternary volcanoes (light lines). The effective repository area, A_e, is 5.49 km^2.

Figure 5. Annual probability of volcanic eruptions within the repository boundary. Volcanic events are defined as vents and vent alignments. A Gaussian kernel is used with smoothing parameter, *h*, of 5 and 7 km (labeled lines) and is based on the distribution of three Quaternary volcanic events (Quaternary Crater Flat alignment, Sleeping Butte alignment, and Lathrop Wells cinder cone). Analysis of existing vent distribution indicates $h \geq 7$ km is suitable for volcanic hazard analysis at the repository. Vent alignment half-length, l_{max}, varied between 5,200 and 10,200 m, roughly changing probability estimates by a factor of two. Probabilities are calculated using $\lambda_t = 3 \times 10^{-6}$/yr.

Figure 6. The weighting function, $f_T(x,y)$, is derived from average crustal densities at Plio-Quaternary volcanoes. These densities are estimated from regional gravity data [*Connor et al.*, 1986b].

Figure 7. The spatial weighting factor (v/km^2) is contoured in the area of Yucca Mountain, using the Gaussian kernel function [equation (13)]. In this model, h = 9,000 m and N = 3, based on the number of Quaternary volcanic events, as in Figure 6. The contour interval is 2×10^{-4} v/km^2. Other map symbols are as in Figure 1.

Figure 8. The spatial weighting factor (v/km^2) is contoured in the area of Yucca Mountain, using the modified Gaussian kernel function [equations (23)–(24)] to incorporate tectonic control on the probability estimate. In this model, h = 9,000 m and N = 3, based on the number of Quaternary volcanic events, as in Figure 6. The contour interval is 2×10^{-4} v/km^2. Other symbols are as in Figure 1.

Figure 9. Annual probability of volcanic eruptions within the repository boundary. Events are defined as vents and vent alignments. A modified Gaussian kernel is used with smoothing parameter, h = 7 km, based on the distribution of three Quaternary igneous events. Analysis of existing vent distribution indicates $h \geq 7$ km is suitable for volcanic hazard analysis at the repository. Vent alignment half-length, l_{max}, varied between 5,200 and 10,200 m, roughly changing probability estimates by a factor of two. Probabilities are calculated using λ_t = 3×10^{-6}/yr. Curves shown are calculated using Plio-Quaternary events, N = 12, and the modified Gaussian kernel and Quaternary events, N = 3, and the standard Gaussian kernel for comparison.

Figure 10. Annual probability of volcanic eruptions within the repository boundary using regional recurrence rates of λ_t = 1×10^{-6}/yr to 5×10^{-6}/yr. Igneous events are defined as vents

and vent alignments. A modified Gaussian kernel is used with smoothing parameter, $h = 7$ km, based on the distribution of three Quaternary igneous events.

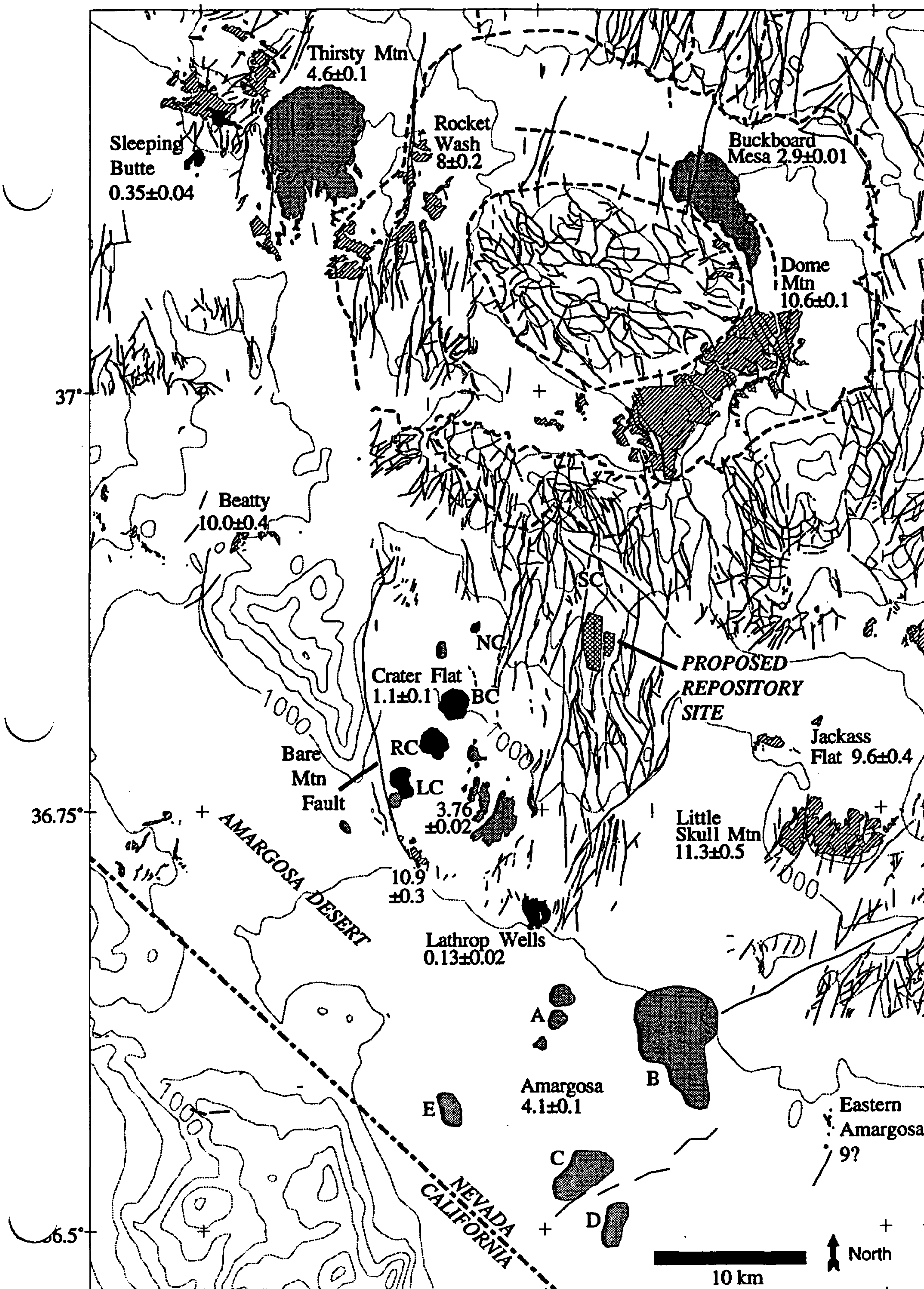

Thirsty Mtn
4.6±0.1
Rocket
Wash
8±0.2
Sleeping
Butte
0.35±0.04
Buckboard
Mesa 2.9±0.01
Dome
Mtn
10.6±0.1
37°
Beatty
10.0±0.4
SC
NC
PROPOSED
REPOSITORY
SITE
Crater Flat
1.1±0.1
BC
1000
RC
Bare
Mtn
Fault
LC
L
3.76
±0.02
Jackass
Flat 9.6±0.4
Little
Skull Mtn
11.3±0.5
36.75°
AMARGOSA DESERT
10.9
±0.3
Lathrop Wells
0.13±0.02
A
B
Amargosa
4.1±0.1
E
Eastern
Amargosa
9?
C
D
NEVADA
CALIFORNIA
36.5°
10 km
North
116.75°
116.5°
116.25°

Fig 1

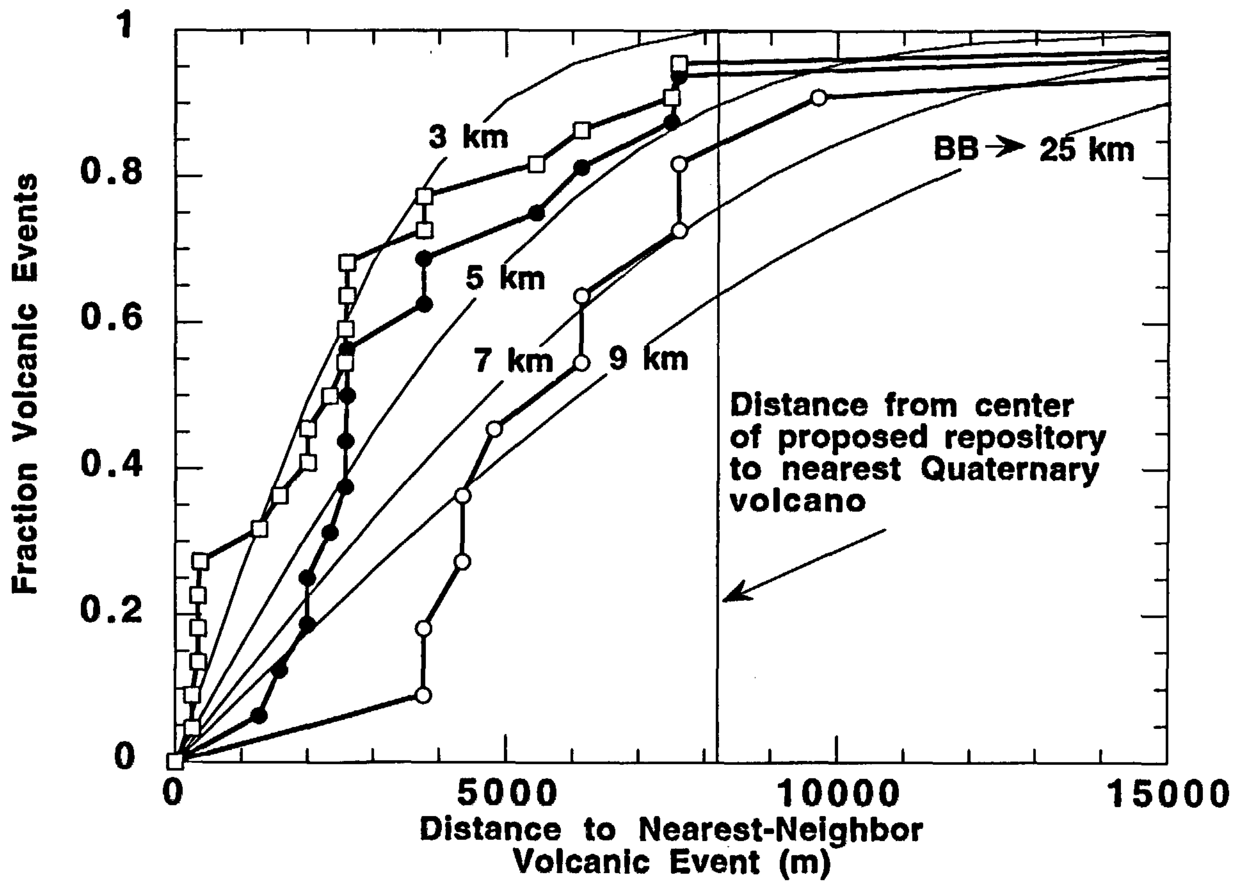
1
0.8
0.6
0.4
0.2
0
Fraction Volcanic Events
0
5000
10000
15000
Distance to Nearest-Neighbor
Volcanic Event (m)
3 km
5 km
7 km
9 km
BB → 25 km
Distance from center
of proposed repository
to nearest Quaternary
volcano

Fig 2

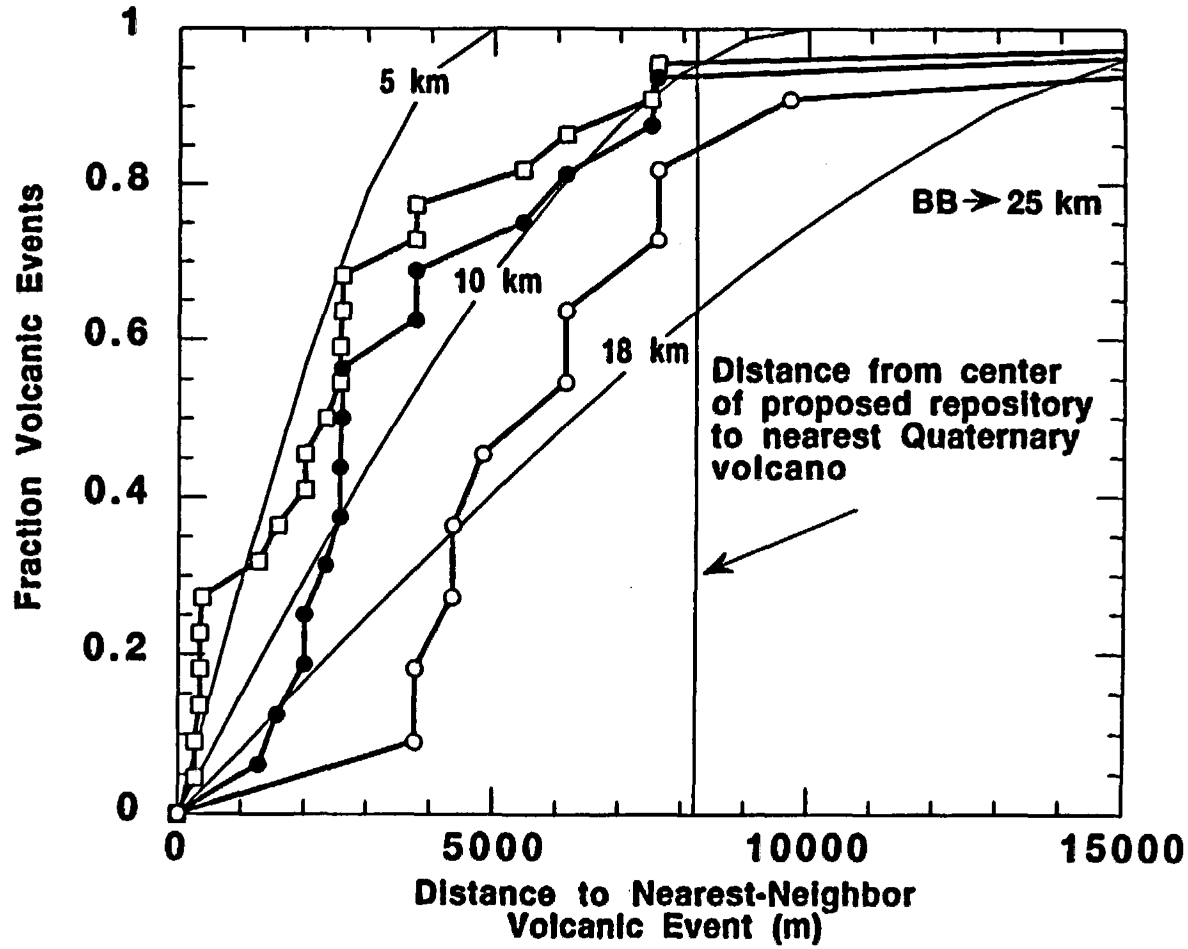
1
0.8
0.6
0.4
0.2
0
Fraction Volcanic Events
5 km
10 km
18 km
BB → 25 km
Distance from center of proposed repository to nearest Quaternary volcano
0
5000
10000
15000
Distance to Nearest-Neighbor Volcanic Event (m)

Fig 3

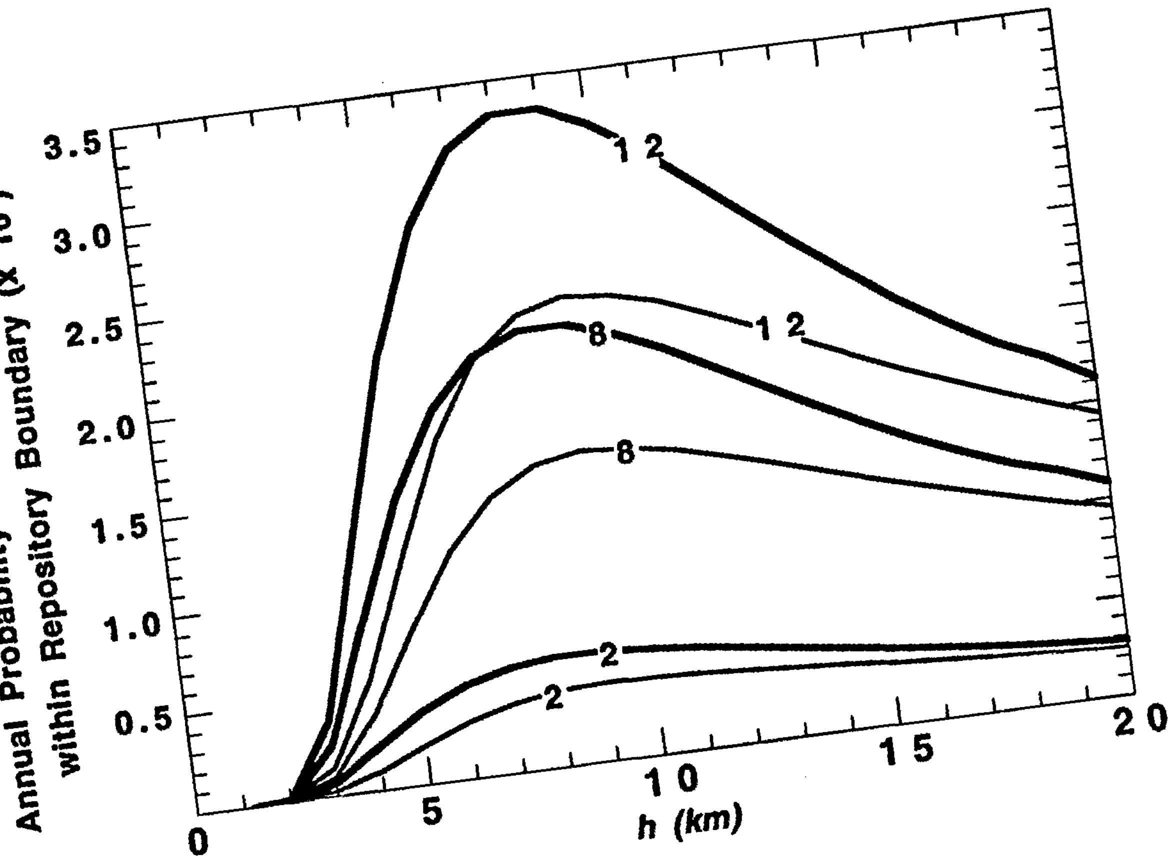

Annual Probability of Volcanic Eruptions within Repository Boundary (x 10^8)
3.5
3.0
2.5
2.0
1.5
1.0
0.5
0
5
10
15
20
h (km)
12
12
8
8
2
2

Fig. 4

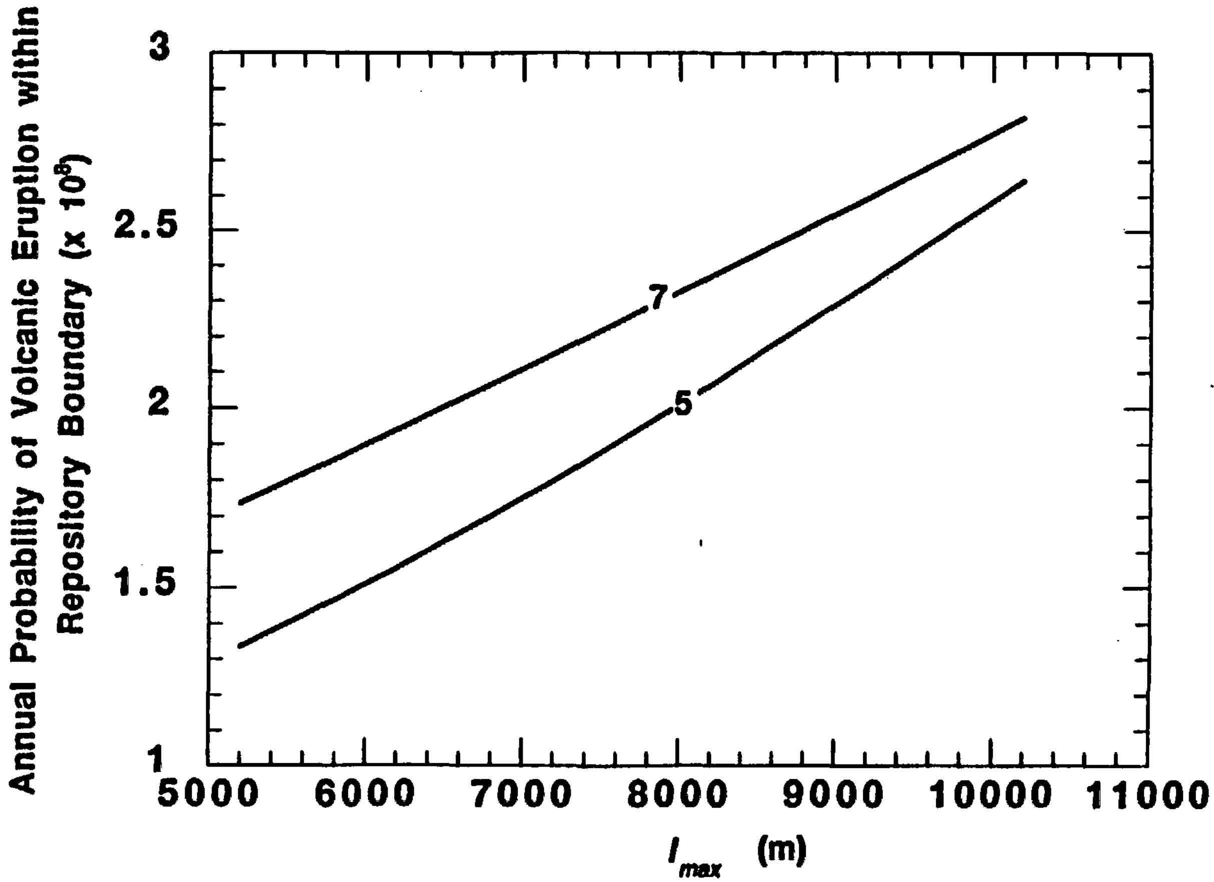
Annual Probability of Volcanic Eruption within Repository Boundary (x 10^8)
3
2.5
2
1.5
1
5000
6000
7000
8000
9000
10000
11000
l_{max} (m)
7
5

Fig 5

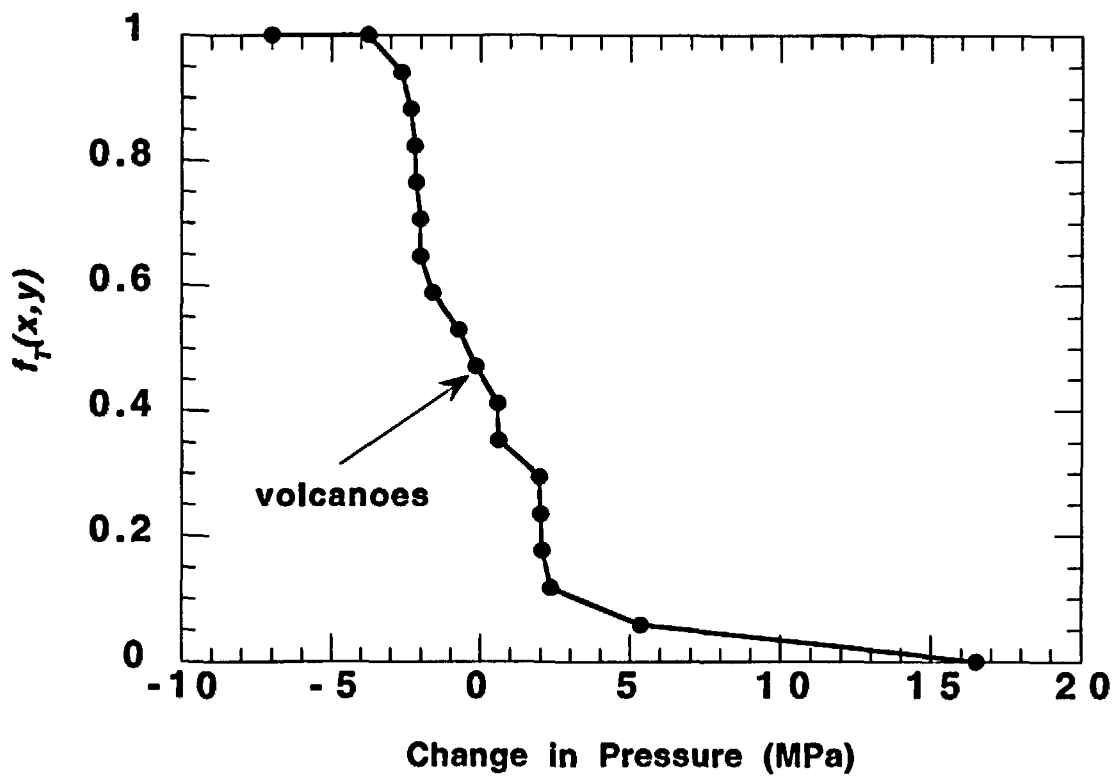
1
0.8
0.6
0.4
0.2
0
$f_T(x,y)$
volcanoes
-10
-5
0
5
10
15
20
Change in Pressure (MPa)

Fig. 6

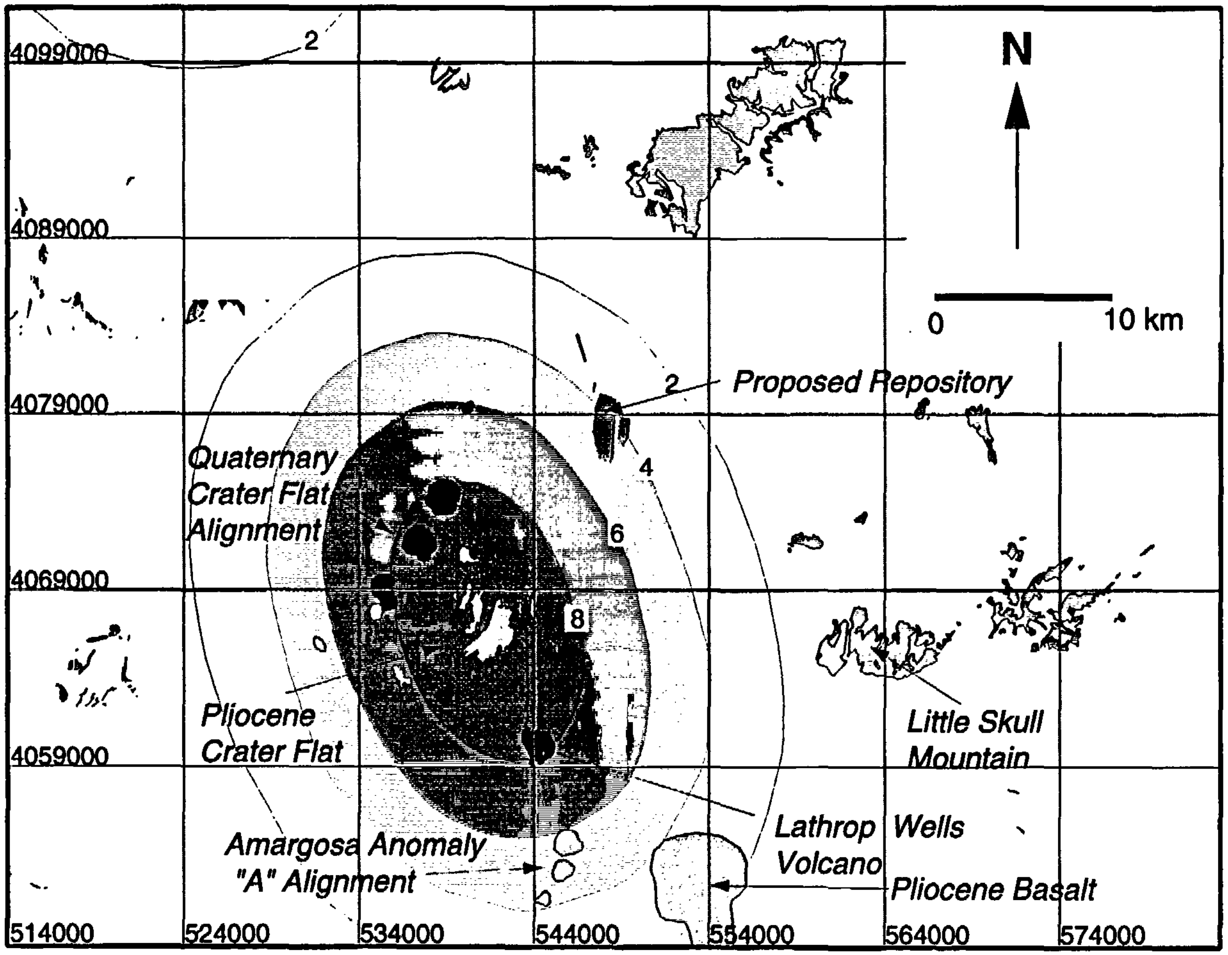
N
0
10 km
4099000
4089000
4079000
4069000
4059000
514000
524000
534000
544000
554000
564000
574000
2
2
4
6
8
Proposed Repository
Quaternary Crater Flat Alignment
Pliocene Crater Flat
Little Skull Mountain
Lathrop Wells Volcano
Amargosa Anomaly "A" Alignment
Pliocene Basalt

Fig 7

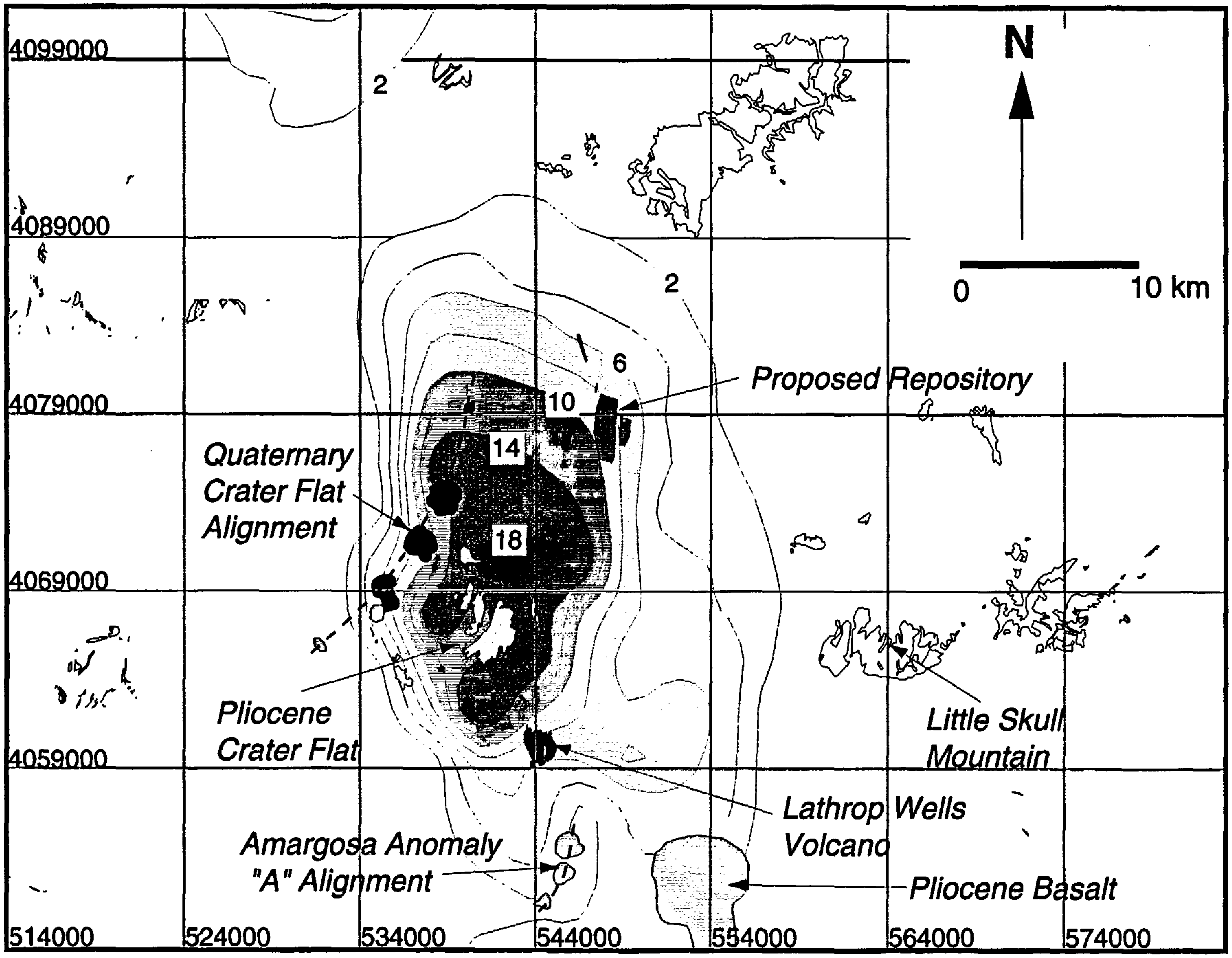
N
0
10 km
4099000
4089000
4079000
4069000
4059000
514000
524000
534000
544000
554000
564000
574000
2
2
6
10
14
18
Proposed Repository
Quaternary Crater Flat Alignment
Pliocene Crater Flat
Little Skull Mountain
Lathrop Wells Volcano
Amargosa Anomaly "A" Alignment
Pliocene Basalt

Fig 8

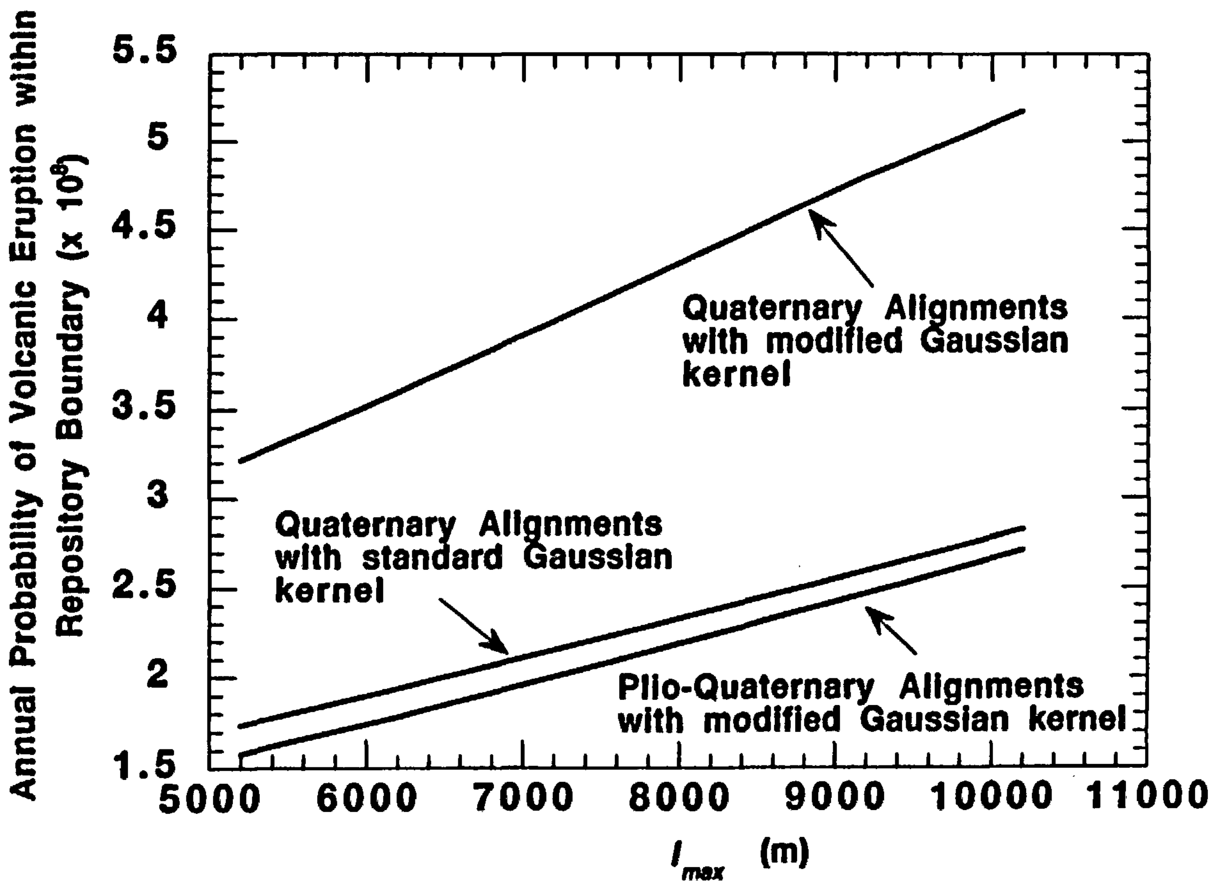
Annual Probability of Volcanic Eruption within Repository Boundary (x 10^{8})
5.5
5
4.5
4
3.5
3
2.5
2
1.5
5000
6000
7000
8000
9000
10000
11000
l_{max} (m)
Quaternary Alignments with modified Gaussian kernel
Quaternary Alignments with standard Gaussian kernel
Plio-Quaternary Alignments with modified Gaussian kernel

Fig 9

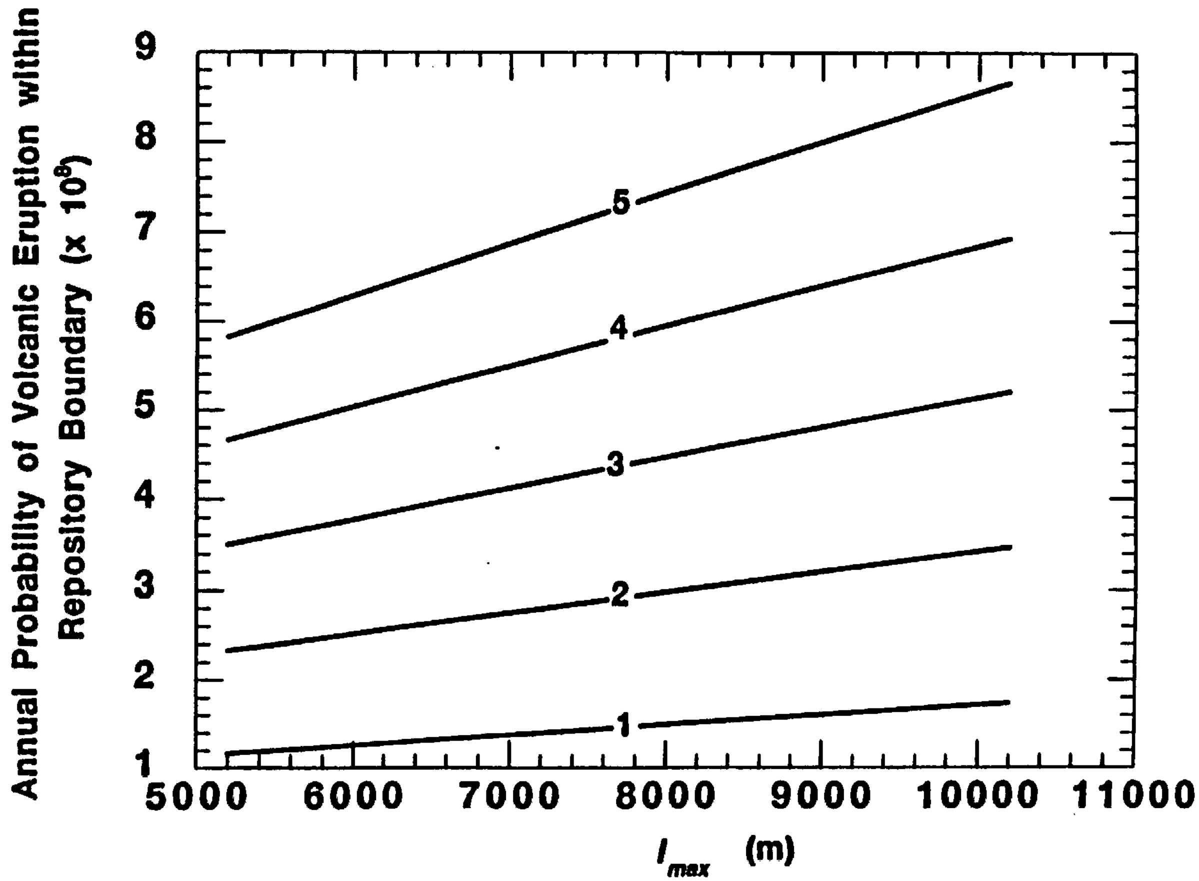
Annual Probability of Volcanic Eruption within
Repository Boundary (x 10^8)
9
8
7
6
5
4
3
2
1
5000
6000
7000
8000
9000
10000
11000
l_max (m)
5
4
3
2
1

Fig 10